Journal of Engineering and Applied Sciences 14 (Special Issue 8): 10305-10310, 2019
ISSN: 1816-949X

Photocatalytic Activity and Electrical Properties of Polypyrrole/Nb_2O_5/Graphene Nanocomposite: Synthesis and Characterization using Hydrothermal Method

Alaa F. Hassen and Nada Y. Fairroz
Department of Chemistry, College of Science, University of Babylon, Hilla, Iraq

Abstract: This investigation was synthesis of the four types (A, B, C, D) of polypyrrole /Nb_2O_5/graphene nanocomposite at different percentage as photo catalyst. The synthesis was by hydrothermal method and polymerization (0.05, 0.1, 0.15, 0.2 g) Nb_2O_5/graphene with 0.6 M pyrrole and drying at temperature 60°C for 24 h. The synthesis nanoparticle by using hydrothermal and calcination at temperatures 700°C for 2 h. Synthesis powders were characterized by AFM, Raman, PET, PJH, XRD, FT-IR, UV-visible and band gap. The photocatalytic activity and electrical properties were studied estimated under high pressure mercury lamp osram (125 wt.) for degradation acridine orange solution at the wave length of 477 nm. It is found the optimum mass catalyst D at 0.2 g and optimum concentration of 20 ppm, the optimum pH 7, temperature 25°C. The X-Ray studies showed the crystal size of composite in the range 4-54 nm. The electrical properties shows in the nanoparticle and poly pyrrole is found weak conductivity and catalyst (A, B, C, D) is higher conductivity.

Keywords: Polypyrrole, nanocomposite, hydrothermal method, synthesis, electrical properties, acridine orange

INTRODUCTION

Nanotechnology mentions to any technology has uses in real world that is implemented at the nanoscale (Zach *et al*., 2006). The material can be re-structured and re-controlled through molecular and atomic levels in the size range of about 1-100 nm. Nanoscience refers to basic science (Barth *et al*., 2010). In the nanoscale the properties of the material differ from those found in a bigger scale. When the dimension of a materials are reduced from a large size, at first, the properties remain as they are and then lesser changes will occur. Finally, when the size drops below 100 nm, dramatic changes in properties can occur (Marques *et al*., 2012). In commercial applications and new structures that benefit society the unique physical and chemical properties of nanomaterials can be exploited. Innovative nanomaterials and nanomaterials can also be developed through nanotechnology the discovery of processes, novel materials and phenomena at the nanoscale and the development of theoretical techniques and new experimental theoretical techniques for research at the end of the 20th century provide fresh opportunities. This field is opening new avenues in science and technology (Faber *et al*., 2005). Ppy is one of the most important conducting polymers for super capacitor applications. Graphene is emerging as an excellent electrode material (Liu *et al*., 2010). Depending on synthesis temperature that includes pseudo-hexagonal (500°C), orthorhombic 600-800°C, metastable (Nikishina *et al*., 2012). It is found that the orthorhombic Nb_2O_5 (T-Nb_2O_5) is the most favorable phase shown to have excellent electrochemical performance due to enhanced reversible capacity have investigated the variation of electrochemical performance with the change in crystal structure of Nb_2O_5 (Zhang *et al*., 2015). Acridine orange dye is widely used in the fields of printing and leather industry lithography and printing ink as well as is a dye containing nitrogen atoms and being heterogeneous (Lu *et al*., 2013). It is also used in biological spots on a wider scale. Indicate that amino acridine has mutagenic potential. The dramatic source of water pollution and disturbance in aquatic life is the release of these colored wastewater into the ecosysteme (Maron and Ames, 1983).

MATERIALS AND METHODS

Experimental: In the synthesis of poly pyrrole Nb_2O_5/ graphene following chemicals were used without further purficiation the chemicals (pyrrole, $Nbcl_5$, $Fecl_3$, ethanol graphite and deionized water).

Prepared of Nb_2O_5/graphene: The prepared first graphene oxide by hummer method and the synthesized nanoparticles by using hydrothermal method by using 15 mL of ethanol and 0.9 g of $Nbcl_5$ at for sonication at 30 min. The prepared the graphene oxide suspension 15 mL of deionized water, 0.045 g of graphene oxide. The mix solutions at worked sonication instrument at 2 h. The last solutions in autoclave at 160°C and 12 h. The filtration of solutions and annealing at 700°C for 2 h to found Nb_2O_5 anchored graphene Nanosheets.

Corresponding Author: Alaa F. Hassen, Department of Chemistry, College of Science, University of Babylon, Hilla, Iraq

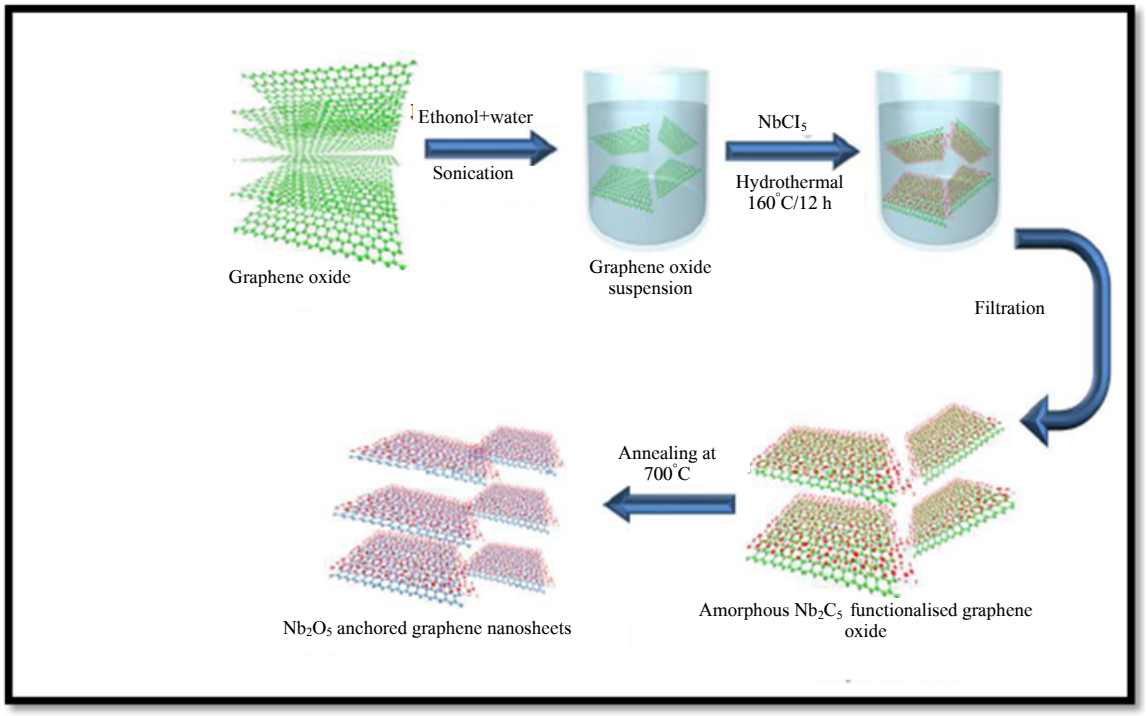

Fig. 1: Schematic illustration of the synthesis of Nb_2O_5 anchored nanocomposite through hydrothermal method

Synthesis of poly pyrrole/Nb_2O_5/graphene: Nb_2O_5/graphene at different weights (0.05, 0.1, 0.15, 0.2) were dispersed in o.6 M of $FeCL_3$. $6H_2O$ at 30 h 0.2 mole of pyrrole was added drop to drop to last mix at stirring 3 h. Filtaration the suspension draying the precipitate at the oven 60°C for 24 h (Kepeniene *et al*., 2018) (Fig. 1).

RESULTS AND DISCUSSION

Among these for types of nano composite we choice catalyst (D) as the better one compare to the other (A, B, C, D) due the higher efficiency through the result (Fig. 2).

UV/Visible spectroscopy: To study the degradation of the acridine orange dye on the composite (D) as well as the determination of the maximum wavelength of the orange acridine dye was used T80 UV-Vis spectrophotometer double beam shiatsu UV-1800 UV spectrophotometer serial No. (AU 454806500) (Fig. 3).

XRD: Mass symmetrical is important in exploring the optical, structural and electrical properties of nanoparticles in order to evaluate crystalline structure and distance and network parameters. The result of single polypyrrole /Nb_2O_5/graphene is affirmed in the wake of breaking down the XRD diffraction pattern. The crystal

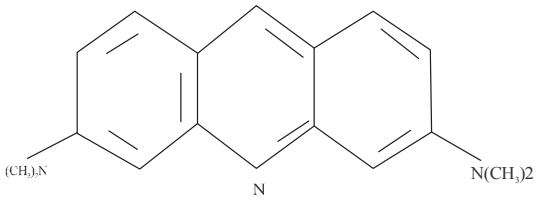

Fig. 2: Structure of acridine orange dye

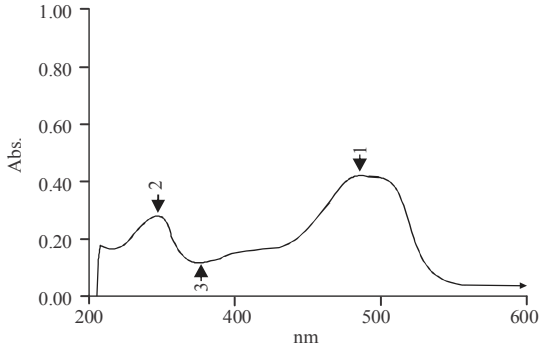

Fig. 3: UV/Visible spectrum of acridine orange dye

structure is observed to be cubic with space gathering. Figure 4 show the XRD diffractions patterns of polypyrrole and nanocomposite and composite having different composition (A = 0.05-B = 0.1-C =

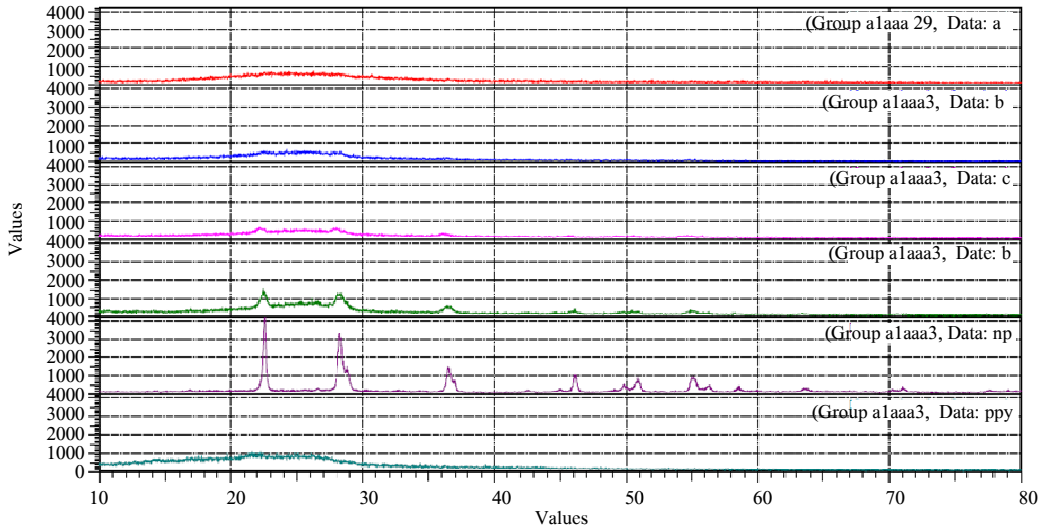

Fig. 4: XRD patterns of poly pyrrole, nanoparticle, catalyst A, B, C and D

Table 1: Particles size of PPY, NP, A, B, C, D

Samples	2θ	FWHM	Crystal size (nm)
Nb_2O_5/graphene	22.13710	0.18000	54.35
	50.83530	0.32500	48.11
	77.61080	0.43670	41.38
Polypyrrole ppy	21.99740	2.08000	3.11
	50.92781	0.80000	2.75
	77.87910	0.40000	2.37
Catalyst A	22.75570	1.08000	4.00
	51.28570	0.12000	3.58
	78.24900	0.26000	3.01
Catalyst B	22.64590	1.18000	8.00
	62.58350	0.00000	6.79
	77.53920	0.00000	6.19
Catalyst C	28.01110	0.93000	8.19
	50.48800	0.44000	6.52
	77.28930	0.14000	6.20
Catalyst D	22.49480	0.56290	7.79
	37.19600	0.00000	7.53
	78.88880	0.26000	6.13

0.15-D = 0.2). The particle size, 2θ° and FWHM (deg) are shown in Table 1 the particle size is calculated by utilizing the equation Debye:

$$D = k\lambda/\beta\cos$$

Figure 4 shows the X-ray pattern of polypyrrole we find that the nature of polypyrrole is amorphous because all the peaks at the lower diffraction anyles 23-001 are wide and this is why the expansion peaks are can be ascribed to the scattering of the ppy chains at the inter planner spacing (Webb *et al*., 2016) crystalline structure of synthesized Nb_2O_5/graphene was obtained with by using hydrothermal method and small diffraction peak at 22.5 for Nb_2O_5/graphene is attributed to the distordered sheets which overlap with 001 and 28.5 for 041 and 37 this low intense broad band also reveals the presence of highly disordered graphene sheets with no exidence of restacking of individual sheets. Composite A, B, C and D for the crystal weak.

Fourier transform infrared spectroscopy: The infrared spectra of poly pyrrole show the band C = C at 1544.98 cm^{-1} and C-C at 1467.83 cm^{-1} and polypyrrole show C-N at 1170.79 cm^{-1} and C-H at 1089.78 cm^{-1} of pyrrole stretching vibration and Nanoparticle (NP) shows the band C = C at 1548.84 cm^{-1} and C-C at 1467.83 cm^{-1} and composite (A, B, C, D) were performed in the (400-3500 cm^{-1}) range. The FT-IR result show broadening and shifts of peaks to words lower wave number in all composites samples suggesting better conjugation and some chemical interaction between poly pyrrole and Nb_2O_5/graphene nanoparticles.

Atomic force microscopy: For morphological analysis the surface technique is used AFM. Allowing us to arrange individual atoms or particles in the structure as well as to see and measured the surface structure with higher reliability. Resutls shows the mean grain size of ppy at 70 nm and area roughness at 154.5 pm^2 and the mean grain size of nanoparticle at 66 nm and area roughness at 618 pm^2 and the mean grain size of catalyst D at 89 nm and area roughness at 2.472 nm^2 (Eaton and West, 2010).

(Dielectric constant measurements): Results show the imaginary and real permittivity versus log frequency of nanocomposite and composite, individually increased with decrease frequency. The estimate performed at room temperature as the electrical fields frequency increased. The greater dipolar makes difficult to fix a distinguish speed from the exchanging field hence the commitment of these dipolar gathering to the permittivity

continues diminishing bringing a persistently decreasing permittivity of catalyst D at higher frequency.

Electric measurement of poly pyrrole and nanocomposite and catalyst D: Results shows the conductivity of poly pyrrole and nanoparticle is weak but conductivity of catalyst (A, B, C, D) is high because all of crystalline decrease the conductivity increasing because the prevent self collects present in the polymer and that open the new method of conductivity paths.

Raman analysis: The G and D peaks are the main features in the Raman spectra of graphitic carbon based materials ppy shows the structural changes after the duction of Go the Raman spectra of ppy is generally, characterized by D band at 1400 cm^{-1} (sp-defects originating from disordered carbon) and G band at 1600 cm^{-1} (sp-hybridized graphitic carbon) are observed, suggesting the existence of graphene the intensity ratio of these two bands indicates the quality of the product ID/IG, Results show catalyst (D) band at 1290 cm^{-1} and G band at 1590 cm^{-1}.

BET analysis: The Barret-Joyner-Halenda and BET (Brunauer-Emmett-Tellerften) when taking into account the effects of fine crystals and predicting the size of pores and determine them in a stable manner on the basis of the electron microscope and X-ray radiation the models often fail when distinguishing between the different forms of porous composition. For data analysis, experimental possibilities and new nanomaterials require new theoretical methods were the first to use the DFT method to calculate the parameters of a porous structure from the adsorption isotherms. Seaton *et al*., the world Lastoskie et al of has done an improvement for this way results shows the surface area of single point isotherm for nanoparticle to 15.7722 m^2g^{-1} and multipoint for 16.072 m^2g^{-1} and multi-point of slope at 215.300 and intercept at 1.377e+00 and correlation coefficient at 0.999822 and constant at 157.349 the surface area of poly pyrrole of single point isotherm to 9.3879 m^2g^{-1} and multipoint for 13.032 m^2g^{-1} and multi-point of slope at 210.605 and intercept at 5.662e+01 and correlation coefficient at 0.999610 and constant at 4.719. The surface area of catalyst D of single point isotherm for 19.0702 m^2g^{-1} and multipoint for 36.917 m^2g^{-1} and multi-point of slope at 46.045 and intercept at 4.829e+01 and correlation coefficient at 0.999007 and constant at 1.954 (Bhushan *et al*., 2014).

BJH analysis: To determine the volume, size and distribution of pores in adsorbents most of the time this is done through the use of a method developed by Barrett-Joyner-Halenda (BJH). The phenomenon of capillary condensation takes place in mesopores (the gas is adsorbed in the pores as liquid at pressures close to (but below) the equilibrium vapour pressure) it is based on the assumption that within the relative pressure range of 0.4 <p/p0<0.98. The reason for increasing the thickness of the absorbent layer on the walls of the pores is to increase the pressure. Results shows the surface area of nanoparticle for 16.083 m^2g^{-1} and pore volume at 0.064 ccg^{-1} and pore diameter (d) at 2.455 nm. The surface area of poly pyrrole for 18.427 m^2g^{-1} and pore volume at 0.031 ccg^{-1} and pore diameter at 3.079 nm. The surface area of catalyst D for 43.050 (m^2g^{-1}) and pore volume at 0.076 ccg^{-1} and pore diameter at 3.078 nm.

Photo-catalytic degradation

Effect of catalyst mass: The effect of photo degradation of orange acardine was studied by taking different weights (0.05, 0.01, 0.03, 0.1, 0.15, 0.2) g with 10 ppm of the catalyst D under ultraviolet light at 25°C for 60 min. results show the increase in the number of active sites available on the surface of the catalyst D to react to obtain a high amount of catalyst is more than 0.2 g due to the increased activity of the catalyst D which leads to the removal of high efficiency of the acridine orange. The increased particle size and decreased in particular surface area which leads to deceased in quantity of surface dynamic locales causing photo degradation efficiency was decreased suitable to an agglomeration, the most effective photo degradation of catalyst (D) was observed with 0.2 g of catalyst weight causing as well high amounts of catalyst lead to increased of light diffusion. This tends to decreased the passing of irradiation through the sample.

Effect of temperature: Using different temperatures for raining (15, 20, 25, 30, 35°C) the process of photo degradation of the catalyst D was measured Fig. 5 shows the effects of different temperature on the photo degradation efficiency of catalyst D at initial concentration 20 ppm and 0.2 g of catalyst D. Also, we can see from the diagram 12 that the efficiency of the photolysis of the catalyst D increases when the temperature increases and optimum temperature 35°C.

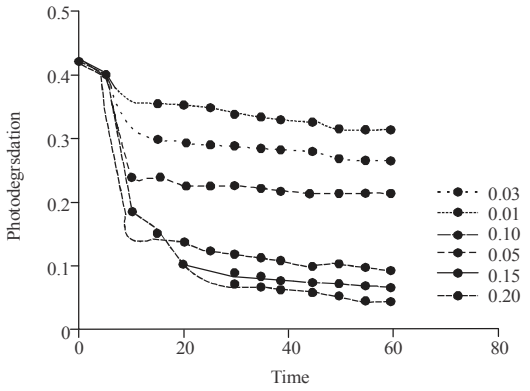

Fig. 5: Effect of the weight of catalyst D

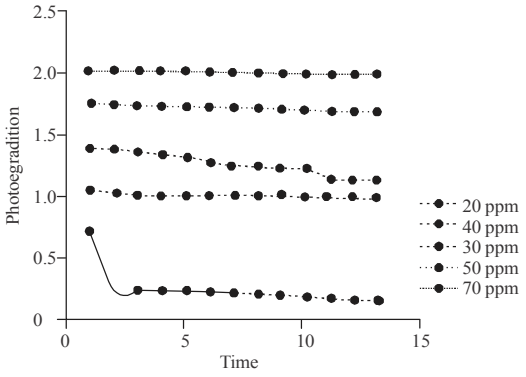

Fig. 6: Effect of the concentration of catalyst D

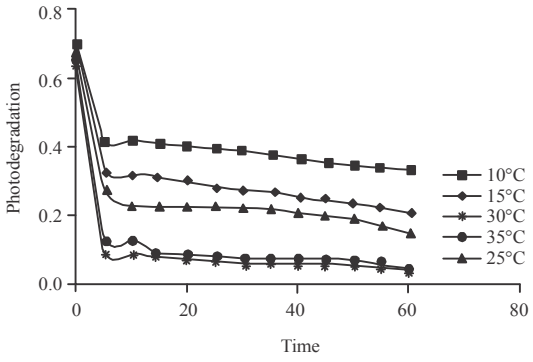

Fig. 7: Effect of the temperature of catalyst D

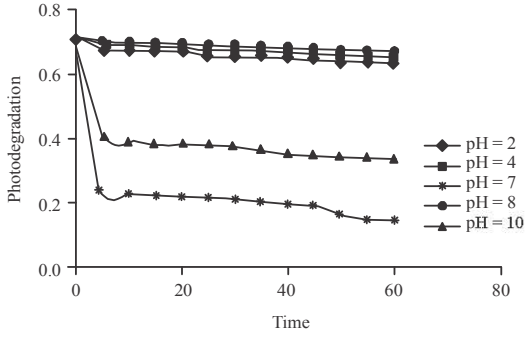

Fig. 8: The effect of pH

Effect of pH: At different pH (2, 4, 7, 8, 10) with 0.2 g of catalyst D with 20 ppm. Figure 6 show the effact of pH it is found optimum pH at pH = 7 and photo degration efficiency increased for pH = 7 and efficiency photo degradation decrease for pH = 10 (Fig. 7 and 8).

CONCLUSION

The research include composite polypyrrole Nb_2O_5/graphene were synthesized by polymerization method and synthesized Nb_2O_5/graphene nanoparticles by hydrothermal method the shows the ability of catalyst D for photocatalytic process is efficiency at 94 at best weight of 0.2 g, the concentration of catalyst 20 ppm, pH 7 the temperature 25°C having radiation time of 60 min. The average particle size of nanoparticles are in the ranges of (4-54 nm). As analyzed by by X-ray diffraction and AFM technique. The conductivity of stander poly pyrrole and nanoparticle is week but composite D is higher conductivity. When frequency increased with conductivity increased.

REFRENCES

Barth, J.V., G. Costantini and K. Kern, 2010. Engineering Atomic and Molecular Nanostructures at Surfaces. In: Nanoscience and Technology: A Collection of Reviews from Nature Journals, Peter, R. (Ed.). World Scientific, Singapore, ISBN-13: 978-981-4282-68-0, pp: 67-75.

Bhushan, B., D. Luo, S.R. Schricker, W. Sigmund and S. Zauscher, 2014. Handbook of Nanomaterials Properties. Springer, Berlin, Germany, ISBN: 978-3-642-31106-2, Pages: 1463.

Eaton, P. and P. West, 2010. Atomic Force Microscopy. Oxford University Press, Oxford, UK., ISBN: 9780199570454, Pages: 248.

Faber, B., J. MacKinnon and M. Petroccione, 2005. Media portraits of nanotech in North American written media: 1986-2000. Nanotech. L. Bus., 2: 348-363.

Kepeniene, V., R. Stagniunaite, L. Tamasauskaite-Tamasiunaite, V. Pakstas and E. Norkus, 2018. $PtCoNb_2O_5$/graphene as electrocatalyst towards oxygen reduction reaction in alkaline and acidic media. Chemija, 29: 41-48.

Liu, C., Z. Yu, D. Neff, A. Zhamu and B.Z. Jang, 2010. Graphene-based supercapacitor with an ultrahigh energy density. Nano Lett., 10: 4863-4868.

Lu, C.S., C.C. Chen, L.K. Huang, P.A. Tsai and H.F. Lai, 2013. Photocatalytic degradation of acridine orange over $NaBiO_3$ driven by visible light irradiation. Catalysts, 3: 501-516.

Maron, D.M. and B.N. Ames, 1983. Revised methods for the Salmonella mutagenicity test. Mutat. Res. Environ. Mutagen. Relat. Subj., 113: 173-215.

Marques, M.A.L., N.T. Maitra, F.M.S. Nogueira, E.K.U. Gross and A. Rubio, 2012. Fundamentals of Time-Dependent Density Functional Theory. Vol. 837, Springer, Berlin, Germany, ISBN: 978-3-642-23518-4, Pages: 559.

Nikishina, E.E., E.N. Lebedeva and D.V. Drobot, 2012. Niobium-and tantalum-containing oxide materials: Synthesis, properties and application. Inorg. Mater., 48: 1243-1260.

Webb, S.M., C.C. Fuller, B.M. Tebo and J.R. Bargar, 2016. Determination of uranyl incorporation into biogenic manganese oxides using X-ray absorption spectroscopy and scattering. Environ. Sci. Technol., 40: 771-777.

Zach, M., C. Hagglund, D. Chakarov and B. Kasemo, 2006. Nanoscience and nanotechnology for advanced energy systems. Curr. Opin. Solid State Mater. Sci., 10: 132-143.

Zhang, H., Y. Wang, P. Liu, S.L. Chou and J.Z. Wang *et al*., 2015. Highly ordered single crystalline nanowire array assembled three-dimensional Nb3O7(OH) and Nb2O5 superstructures for energy storage and conversion applications. ACS. Nano., 10: 507-514.